Bipolar Patient–Specific In Vitro Diagnostic Test Reveals Underlying Cardiac Arrhythmia Phenotype Caused by Calcium Channel Genetic Risk Factor

Rachel Dow, Cindy DeLong, Guihua Jiang, Durga Attili, Jeffery Creech, Rachel Kraan, Katherine Campbell, Prakaimuk Saraithong, Sue O'Shea, Andre Monteiro da Rocha, Melvin G. McInnis, and Todd J. Herron

ABSTRACT

A common genetic risk factor for bipolar disorder is *CACNA1C*, a gene that is also critical for cardiac rhythm. The impact of *CACNA1C* mutations on bipolar patient cardiac rhythm is unknown. Here, we report the cardiac electrophysiological implications of a bipolar disorder–associated genetic risk factor in *CACNA1C* using patient induced pluripotent stem cell-derived cardiomyocytes. Results indicate that the *CACNA1C* bipolar disorder–related mutation causes cardiac electrical impulse conduction slowing mediated by impaired intercellular coupling via connexin 43 gap junctions. In vitro gene therapy to restore connexin 43 expression increased cardiac electrical impulse conduction velocity and protected against thioridazine-induced QT prolongation. Patients positive for bipolar disorder *CACNA1C* genetic risk factors may have elevated proarrhythmic risk for adverse events in response to psychiatric medications that slow conduction or prolong the QT interval. This in vitro diagnostic tool enables cardiac testing specific to patients with psychiatric disorders to determine their sensitivity to off-target effects of psychiatric medications.

https://doi.org/10.1016/j.bpsgos.2024.100296

Bipolar disorder (BD) is an episodic psychiatric disorder characterized by alternating manic episodes and depressed episodes. Genome-wide association studies that have included large numbers of patients with BD and control participants have consistently identified single nucleotide polymorphisms (SNPs) in the *CACNA1C* genetic locus that are considered to be a high-risk genotype for BD and schizophrenia (1–4). *CACNA1C* SNPs are also associated with inherited cardiovascular diseases such as Timothy syndrome and other arrhythmias (5–7). *CACNA1C* encodes the pore-forming α1C subunit of the L-type voltage-gated calcium channel, also referred to as the Cav1.2 α1C subunit. It is unknown whether the same BD genetic risk factor (*CACNA1C* SNP) also predisposes to cardiac arrhythmias in these patients.

Here, our goal was to determine the impact of a *CACNA1C* SNP associated with BD on the human cardiac system. Bipolar patient heart tissue is not readily available for research, so we turned to utilizing bipolar patient–specific human induced pluripotent stem cell-derived cardiomyocytes (hiPSC-CMs). hiPSCs were utilized from a patient with BD carrying the disease-associated *CACNA1C* SNP (rs1006737; AA), and in vitro CRISPR (clustered regularly interspaced short palindromic repeats) correction of the *CACNA1C* SNP (corrected to GG) was done to generate an isogenic control line for direct

determination of the SNP effect on cardiac phenotypes. Interestingly, the rs1006737 *CACNA1C* SNP is also associated with cardiovascular comorbidity and increases the risk for developing essential hypertension (8,9). In the brain, this *CACNA1C* SNP is associated with decreased L-type calcium channel expression, indicating a loss of function of the calcium channel (10). However, the mechanism of action of this *CACNA1C* SNP on cardiac function is unknown. High-throughput cardiac electrophysiology recordings enabled determination of the pathogenic functional impacts of the *CACNA1C* SNP on bipolar patient cardiac rhythm and cardiac protein expression. This in vitro diagnostic approach enables bipolar patient–specific medication screening to identify patients at risk for cardiac arrhythmias and ensure the cardiac safety of prescribed medications.

METHODS AND MATERIALS

hiPSC Maintenance and Cardiac-Directed Differentiation

hiPSC lines were obtained from the Heinz C. Prechter Bipolar Genetics Repository at the University of Michigan, as reported previously (11). We utilized 1 bipolar patient–specific cell line carrying the *CACNA1C* SNP (rs1006737; AA; termed BP18A) and 1 CRISPR-corrected patient cell line (BP18A-C corrected

to GG). An unrelated control hiPSC line was also used for comparison (19-9-11). One iPSC clone was utilized per isogenic pair (BP18A and BP18A-C), and a total of 4 independent cardiac differentiation experiments were conducted per cell line. Stem cell use was approved by the Human Pluripotent Stem Cell Oversight Committee of the University of Michigan. Cryopreserved vials of hiPSCs were thawed and maintained in stem cell maintenance media as colonies in feeder-free conditions as described previously (12–16). hiPSC monolayer cardiac-directed differentiation was performed using a small molecule-based approach, and CMs were purified using magnetic-activated cell sorting as recently described (17). Purified hiPSC-CMs were plated to form confluent monolayers in 96-well plates (75,000 CMs/well) that were designed for rapid maturation of the CM phenotype (17,18).

hiPSC-CM Phenotype Analysis and In Vitro Gene Therapy

Cardiac electrophysiology function was quantified using fluorescent probes to detect action potentials (APs) (FluoVolt) or intracellular calcium transients (CaTs) (Calbryte520AM) of spontaneously beating hiPSC-CM monolayers (17,19). Electrophysiological parameters were measured using a high-speed (100–200 frames per second) camera to enable visualization and quantification of AP or CaT propagation velocity through each monolayer. APs were measured using a 200 frames per second acquisition rate, and CaTs were measured using 100 frames per second. Action potential measurements were made by visualizing a 6×6 (36 total) array of wells in the 96-well plate, as has been described in detail previously (12,19). Dynamic fluorescence analysis to quantify impulse velocity, beat rate, and transient durations was done using commercially available software (.oeat; StemBioSys Optical Electrophysiology Analysis Tool) (16). Original recordings of spontaneous APs are shown in Supplemental Video S1. Confluent monolayers spontaneously activated throughout each well and enabled quantification of impulse propagation velocity through each well (monolayer). Time-space plots, such as confocal line scans, were used to display the activations over time in row A of a plate from each cell line (Figure 1C, D). Each action potential in Figure 1C, D is represented by a flash of light (white), and the conduction velocity differences are visualized in this way, by the angle of the activation across the well. Slow conduction has a greater slope, and faster conduction appears to be a line of activation that is perpendicular to the long axis of the time-space plots. Due to differences in the spontaneous beat rate, a Fridericia correction was applied for comparison of the AP durations and the CaT durations (CaTDs) as reported previously (20).

At the conclusion of each functional recording, cardiac monolayers were processed for protein biochemistry analysis using Western blot approaches. In each 96-well plate used, 100 μL of Laemmli sample buffer was applied to each well to solubilize all cellular proteins. The contents of 2 wells (200 μL, 150,000 hiPSC-CMs) were combined for each cell line and used for sodium dodecyl sulfate polyacrylamide gel electrophoresis and immunoblotting. Antibody signal for each lane was normalized to total protein in each lane determined by total protein stain using Coomassie blue dye. Protein expression was quantified using densitometry (ImageJ) and normalized by the total protein signal. Primary antibodies were used to detect specific expression of connexin 43 (Cx43) (anti-Cx43 antibody, rabbit polyclonal, Alomone Labs) and the L-type calcium channel (CaV1.2, rabbit polyclonal, Alomone Labs). Adenoviral-based acute gene therapy was applied to increase Cx43 protein expression in hiPSC-CMs (Ad-RFP-mGja1; Vector Biolabs). A variety of gene therapy doses were applied (multiplicity of infection = 0, 0.5, 1.0, 2.5, 5.0, 10.0) to determine effectiveness. Successful mGJA1 acute gene transfer was monitored with live-cell time-lapse imaging using the red fluorescent protein expression (Incucyte, Sartorius).

RESULTS

Each hiPSC line successfully generated functional CMs with characteristic cardiac sarcomere patterning of F-actin (Figure 1A). Cardiac monolayers from each group generated spontaneous APs that propagated throughout each well and enabled quantification of electrical impulse propagation velocity (Figure 1B–H). AP propagation velocity was slowest in the bipolar patient cell line carrying the *CACNA1C* SNP–associated genetic risk factor (Figure 1B, green symbols conduction velocity = 9.75 ± 3.8 cm/s, vs. unrelated control, white symbols conduction velocity = 33.1 ± 8.2 cm/s, and isogenic CRISPR control, red symbols conduction velocity = 30.7 ± 9.2 cm/s). The slow AP conduction velocity associated with the *CACNA1C* SNP is also visible in the time-space plots (Figure 1C, D) of multiple well activations from each group. AP duration 30 was significantly shorter in the *CACNA1C* SNP hiPSC-CMs, indicating loss of function of the calcium channel (Figure 1F). AP triangulation, an index of proarrhythmic potential, was greater in the mutant cells (Figure 1H). Next, we quantified the calcium flux and wave propagation velocity in each group using a different batch of hiPSC-CM differentiated cells. Calcium wave propagation velocity was also slower in the bipolar patient monolayers carrying the *CACNA1C* SNP–associated genetic risk factor (10.93 ± 3.2 cm/s) than in the isogenic CRISPR-corrected monolayers (20.28 ± 5.34 cm/s) (Figure 1J). Accordingly, the intracellular CaT upstroke slope was also slower in the *CACNA1C* SNP cells (Figure 1K). Calcium triangulation-like AP triangulation (21–23), as a marker of proarrhythmic risk, was greater in the *CACNA1C* SNP cells than in the CRISPR-corrected hiPSC-CM monolayers (Figure 1L). The vast differences in cardiac impulse propagation velocity led us to determine the Cx43 gap junction protein expression in each group next. Cx43 protein expression was significantly reduced in the *CACNA1C* SNP cardiac monolayers compared with the CRISPR-corrected monolayers (Figure 1M, N).

Recombinant adenovirus was used for in vitro gene therapy to restore Cx43 protein expression in the bipolar patient *CACNA1C* SNP cardiac monolayers. Live-cell Cx43 expression was monitored for 44 hours using red fluorescent protein expression driven by the cytomegalovirus promoter engineered into the Ad-RFP-mGja1 virus (Figure 2A; Figure S1). The functional effects of the Cx43 gene therapy were recorded 44 hours after virus was applied. Cx43 acute gene transfer restored *CACNA1C* SNP cardiac monolayer calcium release kinetics and impulse propagation velocity to control levels in a
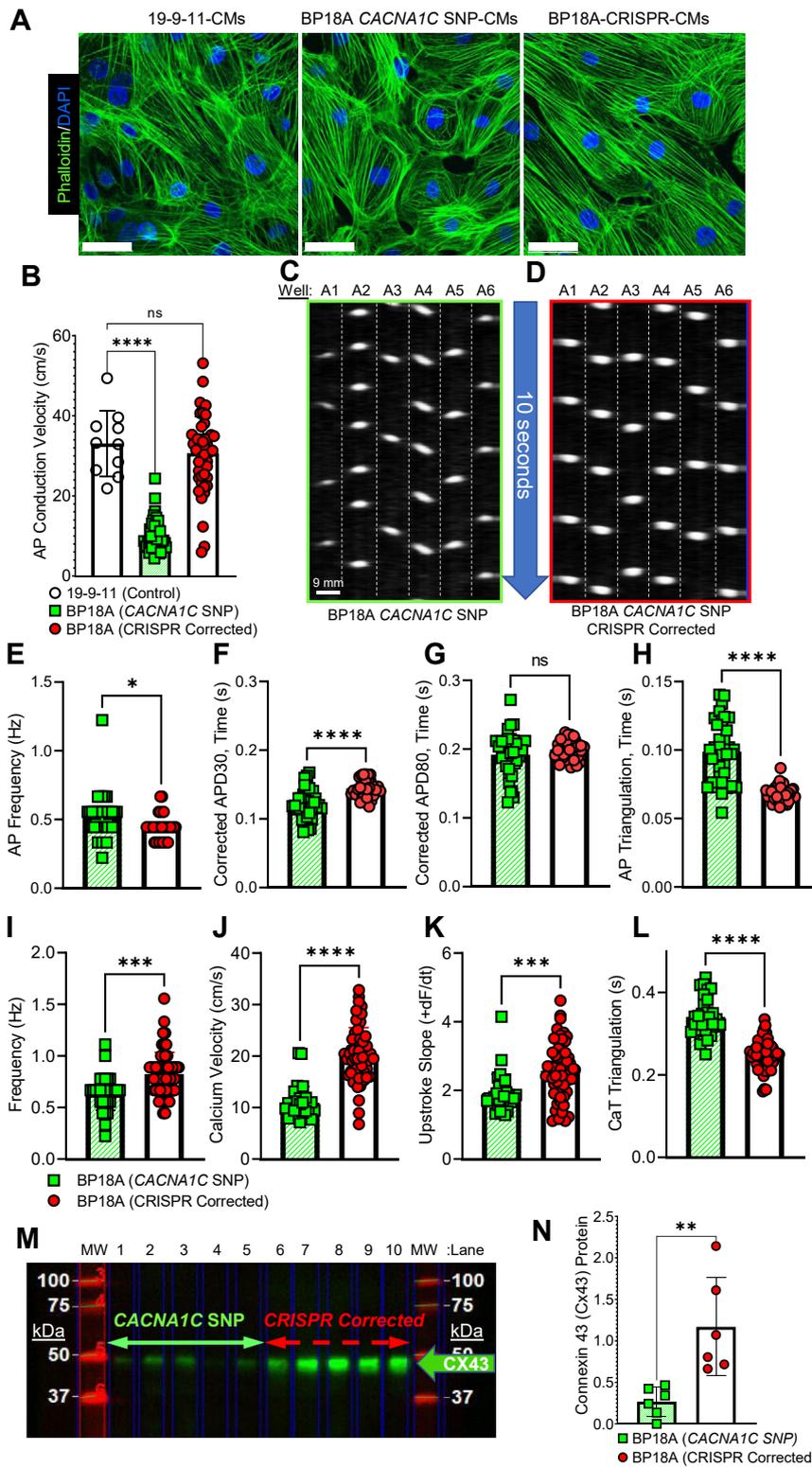
Figure 1. *CACNA1C* SNP is associated with slow cardiac electrical conduction velocity and deficient Cx43 gap junction protein. **(A)** Cytoskeletal staining of F-actin (phalloidin, green) shows sarcomere pattern of localization as expected for human CMs. Blue staining is for the nuclei, white scale bar = 50 μm. **(B)** Cardiac AP conduction velocity was significantly slower in the bipolar patient–specific CMs carrying the *CACNA1C* SNP (9.75 ± 3.8 cm/s; n = 48 monolayers; green symbols) than in the CRISPR-corrected cells (30.7 ± 9.2 cm/s; n = 48 monolayers; red symbols) and unrelated patient control monolayers (33.1 ± 8.2 cm/s; n = 10 monolayers; white symbols; 1-way analysis of variance, ****$p < .0001$). **(C)** Time-space plot shows 10-second recordings of spontaneous activations over 6 separate monolayers (6 separate wells of a 96-well plate) in the bipolar patient *CACNA1C* SNP-expressing cells. Each flash of light represents an individual activation in that monolayer. The slanted appearance of each activation indicates slow impulse propagation velocity. **(D)** Time-space plot shows 10-second recordings of spontaneous activations over 6 separate monolayers in the CRISPR-corrected cell line, which is the isogenic control for the *CACNA1C* SNP cells. The activations in the CRISPR-corrected monolayers are not slanted as in **(C)**, which indicates faster conduction velocity. **(E)** AP beat frequency was different between the 2 groups, and so the APDs were corrected. **(F)** Corrected APD30 was shorter in the *CACNA1C* SNP cells (0.122 ± 0.02 s, n = 36 vs. 0.145 ± 0.02 s, n = 32; ****unpaired *t* test, $p < .0001$). **(G)** Corrected APD80 values were not significantly different, however. **(H)** AP triangulation was significantly greater in the *CACNA1C* SNP cells (0.098 ± 0.02 s, n = 36 vs. 0.06 ± 0.006 s, n = 32; ****$p < .0001$). **(I)** Spontaneous beat rate was higher in the CRISPR-corrected monolayers (0.82 ± 0.22 Hz, n = 56) than in the mutant monolayers (0.64 ± 0.17 Hz, n = 30; unpaired *t* test, ***$p = .002$). **(J)** Calcium wave conduction velocity was faster in the CRISPR-corrected monolayers (20.3 ± 5.3 cm/s; n = 56) than in the mutant monolayers (10.9 ± 3.2 cm/s, n = 30; unpaired *t* test, ****$p < .0001$). **(K)** CaT upstroke velocity was faster in the CRISPR-corrected monolayers (+dF/dt = 2.57 ± 0.81, n = 56) than in the mutant monolayers (1.92 ± 0.55, n = 30; unpaired *t* test, ***$p = .0002$). **(L)** CaT triangulation was lower in the CRISPR-corrected monolayers (0.25 ± 0.04 s, n = 56) than in the mutant monolayers (0.34 ± 0.05 s, n = 30; unpaired *t* test, ****$p < .0001$). **(M)** Western blot probing for Cx43 protein expression indicates significantly lower levels of this gap junction protein in the *CACNA1C* SNP mutant monolayers. **(N)** Western blot quantification shows significantly greater Cx43 expression in the CRISPR-corrected monolayers (1.17 ± 0.59 au, n = 6 vs. 0.27 ± 0.18, n = 6 monolayers, unpaired *t* test, **$p = .0051$). AP, action potential; APD, AP duration; CaT, calcium transient; CM, cardiomyocyte; CRISPR, clustered regularly interspaced short palindromic repeats; Cx43, connexin 43; ns, not significant; SNP, single nucleotide polymorphism.
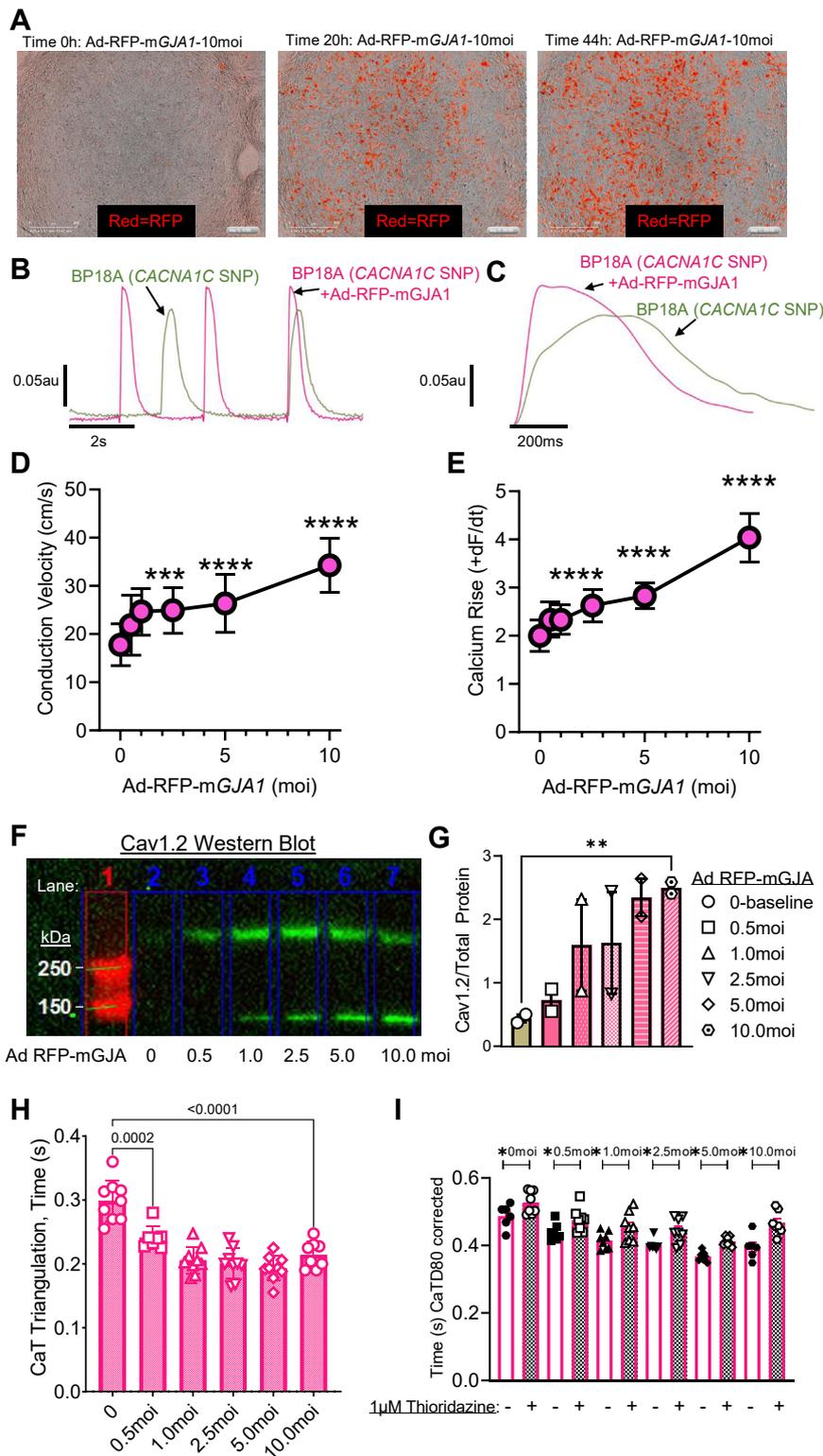
Figure 2. Cx43 gene therapy increases cardiac conduction velocity in bipolar patient cardiomyocyte monolayers expressing the *CACNA1C* SNP. **(A)** Cx43 gene therapy effectiveness was monitored via live-cell time-lapse imaging using RFP as a marker. The number of RFP-positive cells increased over time and was used as a surrogate marker for Cx43 protein expression. Gene therapy was tested using multiple concentrations of virus ranging from 0 to 10 moi as indicated in Figure S1. Scale bar = 800 μm. **(B)** Representative spontaneous CaT traces indicate the functional effects of Cx43 gene therapy over 10-second recordings. **(C)** Aligned single beat traces indicate the increase of calcium rise kinetics induced by Cx43 gene therapy. **(D)** Bipolar patient monolayers harboring the *CACNA1C* SNP conduction velocity could be increased using Cx43 gene therapy. Conduction velocity increased significantly in a gene therapy dose-dependent manner. One-way analysis of variance, multiple comparisons to 0 moi data, ***indicates significant difference from control, 0 moi data, $p = .0004$; ****$p < .0001$. **(E)** Cx43 gene therapy increased the rate of calcium rise/release in a dose-dependent manner. One-way analysis of variance, multiple comparisons to 0 moi data, ****$p < .0001$. **(F)** Western blot analysis for CaV1.2 protein expression indicated low baseline expression in the *CACNA1C* SNP cells, and this expression was restored with Cx43 gene therapy. **(G)** Quantification of Cav1.2 protein expression as a function of Cx43 gene therapy dose indicates significant elevation of L-type calcium channel expression. **(H)** Cx43 gene therapy reduced the calcium triangulation index significantly, unpaired t test values indicated; $p < .05$ indicates significant difference, $n = 7$ to 9 monolayers. **(I)** Cx43 gene therapy reduced the effect of thioridazine (1 μM) to increase CaTD 80, an in vitro surrogate marker for the QT interval of the electrocardiogram. *unpaired t test within each group, $p < .05$, $n = 7$ to 8 monolayers. CaTD, calcium transient duration; moi, multiplicity of infection; RFP, red fluorescent protein; SNP, single nucleotide polymorphism.

virus dose-dependent manner (Figure 2B–E). Restoration of Cx43 expression also reduced CaT triangulation (Figure 2H). Next, we probed for Cav1.2 protein expression to determine whether the Cx43 gene therapy had an impact on the disease gene expression. We found very low-level Cav1.2 protein expression in the BP18A hiPSC-CMs at baseline. The expression of Cav1.2 protein was restored to greater levels with Cx43 gene expression (Figure 2F, G).

Finally, we tested the impact of Cx43 gene therapy on bipolar patient–specific cardiac monolayer responsiveness to the QT-prolonging medication thioridazine (Figure 2I). Thioridazine is a first-generation antipsychotic drug of the phenothiazine group used to treat schizophrenia and psychosis; however, the drug was withdrawn from the market in 2005 due to it causing severe cardiac arrhythmias. Thioridazine binds to and blocks the hERG (the human ether-a-go-go-related gene) potassium channel. Block of the hERG channel is the cellular basis for the negative effects of thioridazine on cardiac rhythm. CaTD at 80% of return to baseline was used as an in vitro surrogate marker for the QT interval of the electrocardiogram. Prolongation of the CaTD can also contribute to diastolic dysfunction and activate calcium-sensitive hypertrophic response genes. Thioridazine (1 μM) prolonged CaTD in the bipolar patient CMs without gene therapy. Cx43 gene therapy reduced the impact of thioridazine to prolong the CaTD (Figure 2I) in the patient cardiac monolayers.

DISCUSSION

CACNA1C has been implicated as one of the strongest genetic associations with BD in genome-wide association studies (24). *CACNA1C* is the gene encoding the L-type calcium channel that is critical for the function of electrically excitable tissues like the brain, pancreas, blood vessels, and heart. BD is also associated with increased risk for cardiovascular disease, including arrhythmias (25). However, the contribution of the BD-associated *CACNA1C* mutation to patient cardiac function is unknown and remains unexplored. Here, we determined the effect of the bipolar patient genetic risk factor *CACNA1C* SNP (rs1006737; AA) on patient cardiac function using hiPSC-CMs monolayers. In control experiments, the *CACNA1C* SNP was corrected to wild-type sequence using CRISPR genome editing technology. Bipolar patient hiPSC-CM monolayers were also compared with hiPSC-CMs that were derived from an unrelated control patient. The *CACNA1C* SNP was found to contribute to cardiac electrical conduction slowing, calcium wave conduction slowing, and increased risk for arrhythmias (Figure 1B–L). Action potential duration shortening was apparent in hiPSC-CMs carrying the *CACNA1C* SNP (Figure 1F) compared to the isogenic control cell line, indicating loss of function of the L-type calcium channel.

Structurally, the BD *CACNA1C* SNP also reduced intercellular Cx43 gap junction protein expression in hiPSC-CM monolayers (Figure 1M, N). Cx43 is the primary gap junction protein in the heart, and reduced expression is known to cause conduction slowing and increased risk for arrhythmias (26). Reduced Cx43 protein expression is a molecular mechanism that can account for the slow conduction velocity and increased arrhythmogenicity indicated by increased AP and CaT triangulation (these are surrogate in vitro markers for

increased QT interval) (23) in the bipolar patient hiPSC-CM monolayers that harbor the *CACNA1C* SNP. The mechanistic relationship between L-type calcium channel gene expression and Cx43 expression is unclear, and future genetic analysis using RNA sequencing or proteomic analysis is warranted. These findings provided a rationale to test the hypothesis that in vitro Cx43 gene therapy improves bipolar patient cardiac monolayer function. Loss of function of the L-type calcium channel may have other effects on cardiac function, including altered contractility, altered excitation contraction coupling, and overall reduction of intracellular calcium concentrations that may impact calcium-sensitive gene expression.

In vitro gene therapy using recombinant adenovirus to restore Cx43 protein expression levels restored hiPSC-CM monolayers' conduction velocity to normal values (Figure 2B–E). Cx43 gene therapy was also antiarrhythmic for the bipolar patient cardiac monolayers as indicated by significant reduction of CaT triangulation with increasing gene therapy dose (Figure 2H). Structurally, Cx43 gene therapy increased the expression of Cav1.2 protein in the bipolar patient–specific hiPSC-CMs expressing the *CACNA1C* disease-associated SNP (Figure 2F, G). This indicates an interrelationship between myocardial gap junction protein expression and L-type calcium channel protein expression. Finally, we tested the impact of Cx43 gene therapy to mitigate the harmful side effects of thioridazine to prolong the QT interval. Cx43 gene therapy reduced the impact of thioridazine to increase the CaTD (QT interval surrogate).

In short, our work indicates that cardiac intercellular communication is impaired when the BD *CACNA1C* SNP is expressed in human cardiac tissues and may predispose patients to risk of developing fatal cardiac arrhythmias. This in vitro diagnostic tool may be used to determine the cardiac safety of prescribed psychiatric medications in a bipolar patient–specific way. For example, antidepressants or other psychiatric medications that are being considered for a patient can now be screened using the patient's specific cardiac monolayers derived from hiPSCs and thereby provide patient-specific risk assessment for potential QT prolongation or proarrhythmia. Patient-specific hiPSC-CM assays also offer the opportunity to determine chronic effects of psychiatric medications on cardiac rhythm, contractile function, and gene expression.

ARTICLE INFORMATION

From the Frankel Cardiovascular Regeneration Core Laboratory, University of Michigan, Ann Arbor, Michigan (RD, JC, RK, PS, AMdR, TJH); Michigan Medicine, Cell and Developmental Biology, University of Michigan, Ann Arbor, Michigan (CD, GJ, DA, KC, SO); Michigan Medicine, Internal Medicine-Cardiology, University of Michigan, Ann Arbor, Michigan (PS, AMdR, TJH); Michigan Medicine, Psychiatry Department, University of Michigan,

Ann Arbor, Michigan (SO, MGM); and Michigan Medicine, Molecular & Integrative Physiology, University of Michigan, Ann Arbor, Michigan (TJH).

Address correspondence to Todd J. Herron, Ph.D., at toddherr@umich.edu.

REFERENCES

1. Khalid M, Driessen TM, Lee JS, Tejwani L, Rasool A, Saqlain M, *et al.* (2018): Association of CACNA1C with bipolar disorder among the Pakistani population. Gene 664:119–126.
2. Moon AL, Haan N, Wilkinson LS, Thomas KL, Hall J (2018): *CACNA1C*: Association with psychiatric disorders, behavior, and neurogenesis. Schizophr Bull 44:958–965.
3. Ferreira MA, O'Donovan MC, Meng YA, Jones IR, Ruderfer DM, Jones L, *et al.* (2008): Collaborative genome-wide association analysis supports a role for ANK3 and *CACNA1C* in bipolar disorder. Nat Genet 40:1056–1058.
4. Orrù G, Carta MG (2018): Genetic variants involved in bipolar disorder, a rough road ahead. Clin Pract Epidemiol Ment Health 14:37–45.
5. Napolitano C, Timothy KW, Bloise R, Priori SG (1993): *CACNA1C*-related disorders. In: Adam MP, Feldman J, Mirzaa GM, Pagon RA, Wallace SE, Bean LJH, *et al*., editors. GeneReviews [Internet]. Seattle, WA: University of Washington. Available at: https://www.ncbi.nlm.nih.gov/books/. Accessed March 12, 2024.
6. Antzelevitch C, Pollevick GD, Cordeiro JM, Casis O, Sanguinetti MC, Aizawa Y, *et al.* (2007): Loss-of-function mutations in the cardiac calcium channel underlie a new clinical entity characterized by ST-segment elevation, short QT intervals, and sudden cardiac death. Circulation 115:442–449.
7. Ozawa J, Ohno S, Saito H, Saitoh A, Matsuura H, Horie M (2018): A novel *CACNA1C* mutation identified in a patient with Timothy syndrome without syndactyly exerts both marked loss- and gain-of-function effects. HeartRhythm Case Rep 4:273–277.
8. Ou X, Crane DE, MacIntosh BJ, Young LT, Arnold P, Ameis S, Goldstein BI (2015): *CACNA1C* rs1006737 genotype and bipolar disorder: Focus on intermediate phenotypes and cardiovascular comorbidity. Neurosci Biobehav Rev 55:198–210.
9. Zhang H, Pushkarev B, Zhou J, Mu Y, Bolshakova O, Shrestha S, *et al.* (2021): *CACNA1C* rs1006737 SNP increases the risk of essential hypertension in both Chinese Han and ethnic Russian people of North-East Asia. Med (Baltim) 100:e24825.
10. Gershon ES, Grennan K, Busnello J, Badner JA, Ovsiew F, Memon S, *et al.* (2014): A rare mutation of CACNA1C in a patient with bipolar disorder, and decreased gene expression associated with a bipolar-associated common SNP of *CACNA1C* in brain. Mol Psychiatry 19:890–894.
11. Chen HM, DeLong CJ, Bame M, Rajapakse I, Herron TJ, McInnis MG, O'Shea KS (2014): Transcripts involved in calcium signaling and telencephalic neuronal fate are altered in induced pluripotent stem cells from bipolar disorder patients. Transl Psychiatry 4:e375.
12. da Rocha AM, Creech J, Thonn E, Mironov S, Herron TJ (2020): Detection of drug-induced torsades de pointes arrhythmia mechanisms using hiPSC-CM syncytial monolayers in a high-throughput screening voltage sensitive dye assay. Toxicol Sci 173:402–415.
13. Davis J, Chouman A, Creech J, Monteiro da Rocha A, Ponce-Balbuena D, Jimenez Vazquez EN, *et al.* (2021): In vitro model of ischemic heart failure using human induced pluripotent stem cell-derived cardiomyocytes. JCI Insight 6.
14. Herron TJ, Rocha AMD, Campbell KF, Ponce-Balbuena D, Guerrero-Serna G, *et al.* (2016): Extracellular matrix-mediated maturation of human pluripotent stem cell-derived cardiac monolayer structure and electrophysiological function. Circ Arrhythm Electrophysiol 9:e003638.
15. Jimenez-Vazquez EN, Arad M, Macías Á, Vera-Pedrosa ML, Cruz FM, Gutierrez LK, *et al.* (2022): SNTA1 gene rescues ion channel function and is antiarrhythmic in cardiomyocytes derived from induced pluripotent stem cells from muscular dystrophy patients. eLife 11:e76576.
16. Monteiro da Rocha A, Allan A, Block T, Creech J, Herron TJ (2023): High-throughput cardiotoxicity screening using mature human induced pluripotent stem cell-derived cardiomyocyte monolayers. J Vis Exp 193.
17. Allan A, Creech J, Hausner C, Krajcarski P, Gunawan B, Poulin N, *et al.* (2023): High-throughput longitudinal electrophysiology screening of mature chamber-specific hiPSC-CMs using optical mapping. iScience 26:107142.
18. Block T, Creech J, da Rocha AM, Marinkovic M, Ponce-Balbuena D, Jiménez-Vázquez EN, *et al.* (2020): Human perinatal stem cell derived extracellular matrix enables rapid maturation of hiPSC-CM structural and functional phenotypes. Sci Rep 10:19071.
19. da Rocha AM, Campbell K, Mironov S, Jiang J, Mundada L, Guerrero-Serna G, *et al.* (2017): hiPSC-CM monolayer maturation state determines drug responsiveness in high throughput pro-arrhythmia screen. Sci Rep 7:13834.
20. Blinova K, Dang Q, Millard D, Smith G, Pierson J, Guo L, *et al.* (2018): International multisite study of human-induced pluripotent stem cell-derived cardiomyocytes for drug proarrhythmic potential assessment. Cell Rep 24:3582–3592.
21. Wang L, Kryshtal DO, Kim K, Parikh S, Cadar AG, Bersell KR, *et al.* (2017): Myofilament calcium-buffering dependent action potential triangulation in human-induced pluripotent stem cell model of hypertrophic cardiomyopathy. J Am Coll Cardiol 70:2600–2602.
22. Hondeghem LM, Carlsson L, Duker G (2001): Instability and triangulation of the action potential predict serious proarrhythmia, but action potential duration prolongation is antiarrhythmic. Circulation 103:2004–2013.
23. Lu HR, Whittaker R, Price JH, Vega R, Pfeiffer ER, Cerignoli F, *et al.* (2015): High throughput measurement of Ca++ dynamics in human stem cell-derived cardiomyocytes by kinetic image cytometry: A cardiac risk assessment characterization using a large panel of cardioactive and inactive compounds. Toxicol Sci 148:503–516.
24. Gordovez FJA, McMahon FJ (2020): The genetics of bipolar disorder. Mol Psychiatry 25:544–559.
25. Rossom RC, Hooker SA, O'Connor PJ, Crain AL, Sperl-Hillen JM (2022): Cardiovascular risk for patients with and without schizophrenia, schizoaffective disorder, or bipolar disorder. J Am Heart Assoc 11:e021444.
26. Jongsma HJ, Wilders R (2000): Gap junctions in cardiovascular disease. Circ Res 86:1193–1197.